Chapter III

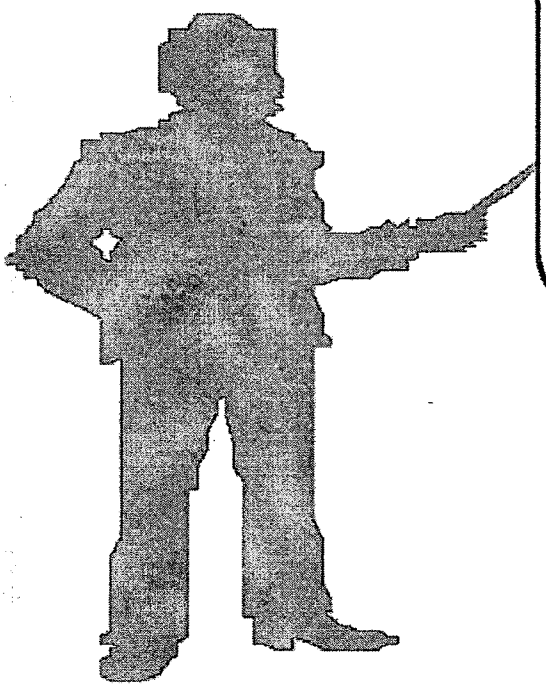

Self-assembly Behavior of Block Copolymer in Aqueous Solution

3.1. Introduction

An increasing interest has been paid to develop liposome-like systems based on block copolymers as competent drug carriers in recent years, with some remarkable, attractive and feasible characteristics (Discher and Eisenberg 2002; Levine et al., 2008; Upadhyay et. al., 2009). Polymer vesicles, also called polymersomes, (Figure 3.1) has became one the most exciting supramolecular self-assembled structures made of block copolymers. Polymersome formation can be achieved in various media such as aqueous solutions (Cornelissen et al., 1998; Discher et al., 1999; Lee James et al., 2001; Li et al., 1999; Schillen et al.,1999; Dimova et al., 2002; Kukula et al., 2002; Checot et al., 2002), non-aqueous solutions (Ding et al., 1997) and mixture of solvents (aqueous and non-aqueous solvent) (Zhang and Eisenberg 1995; Yu and Eisenberg 1998; Shen and Eisenberg 2000; Holder et al., 1998; Nardin et al., 2000). Polymersomes have been proved as an emerging novel carrier for drug delivery (Ahmed et al., 2006) and gene therapy (Kim et al.,2009).

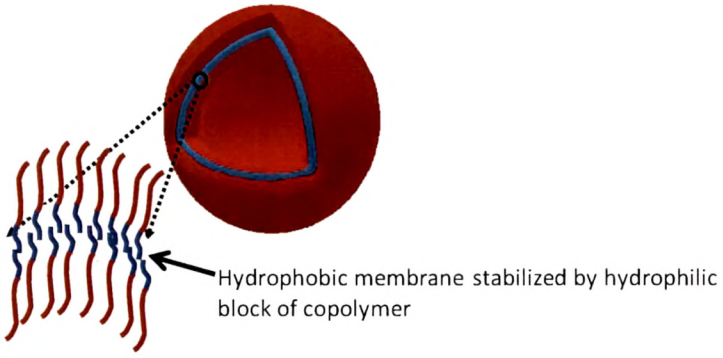

Figure 3.1 Morphology of polymersomes self-assembled from block copolymers.

Among the different parameters having an influence on the self-assembly process, the hydrophilic weight ratio is of high importance as it determines the morphology obtained at the equilibrium. By decreasing this ratio, a transition from spherical micelles to worm micelles and vesicles has been observed (Discher et al., 2000; Burke et al., 2001; Discher and Eisenberg, 2002; Discher et al., 1999; Choucair and Eisenberg, 2003; Yu and Eisenberg 1996; Zhang and Eisenberg 1996). The full mechanism of vesicle formation is described in chapter I. A general method for polymersomes formation, that can be used mainly if the water insoluble block has low Tg, is to directly dissolve the block

copolymer in aqueous media (direct dissolution method) (Schillen et al., 1999; Discher et al., 2000; Upadhyay et al., 2009). Recently, polypeptide-based copolymers were self assembled in peptosomes and polymersomes by direct dissolution of copolymers in an aqueous solution (Kukula et al., 2002; Chécot et al., 2002). If the copolymer is less soluble with high Tg, one has to first dissolve it in a common organic solvent of medium polarity (nonselective solvent), i.e. able to solubilize both blocks, and bringing the polymer solution into aqueous media promotes the self-assembly into polymer vesicles (polymersomes). Subsequently, organic solvent need to be removed by either evaporation or dialysis (Yu and Eisenberg 1998; Yu et al., 1998). This process is called nanoprecipitation or solvent displacement method. For instance, poly(2-methyloxazoline)-*b*-poly(dimethylsiloxane)-*b*-poly(2-methyloxazoline) yielded polymersomes after adding drop wise an ethanolic solution of copolymer in water (Nardin et al., 2000; 2001).

Moreover, polymersomes can also be prepared by thin film hydration which is well known for liposomes preparation. In this method, the copolymer is dissolved in a volatile organic solvent such as chloroform in a glass vial/glass balloon. The solvent is removed by evaporation under a stream of nitrogen gas to leave a thin polymer film, which is rehydrated with the aqueous phase using vigorous stirring, sonication and extrusion to yield submicron vesicles with a narrow size distribution (Discher et al., 1999; Ahmed et al., 2004; Photos et al., 2003).

In comparison with liposomes, polymersomes have many distinct properties. The membrane thickness of polymersomes, which can be controlled by the molecular weight of the hydrophobic block of the copolymer, determines many physicochemical properties such as permeability, and mechanical stability (Discher et al., 1999). Due to the higher molecular weight of the polymers as compared to lipids, the membranes of polymersomes are generally thicker, and therefore, inherently more stable than conventional liposomes.

In this study, we have prepared biodegradable polymersomes from $PBLG_{23}$-*b*-HYA_{10} amphiphilic block copolymer by direct dissolution and nanoprecipitation method. We optimized the procedure of polymersome formation and investigated the influence of

various parameters on the self-assembly process. The morphology of self-assembled $PBLG_{23}$-*b*-HYA_{10} copolymers in aqueous solutions was characterized by static and dynamic light scattering (SLS and DLS), by small angle neutron scattering techniques (SANS), as well as by transmission electron microscopy (TEM) and atomic force microscopy (AFM). In addition, we investigated the lyophilization process on the $PBLG_{23}$-*b*-HYA_{10} based polymersomes.

3.2. Experimental

3.2.1. Polymersomes formation

The formation of polymersomes from $PBLG_{23}$-*b*-HYA_{10} block copolymers was achieved using well-known processes such as the direct dissolution and the so called nanoprecipitation method. *Direct Dissolution*- The block copolymer was dispersed at the concentration of 1 mg/mL in tris buffer (50mM, pH = 7.4) with continuously stirring for 48h at room temperature (RT) or at 40°C. *Nanoprecipitation* - tris buffer (10mM, 154mM ionic strength, pH = 7.4) was injected using a syringe pump with a speed of 18mL/h (5ml syringe) or 36mL/h (10ml syringe), in solution of block copolymer in DMSO (1 wt %) at a final concentration of 1mg/mL. The whole process was achieved at 55°C to favor the polymersomes self-assembly. The organic solvent (DMSO) was removed through the dialysis (MWCO = 2000 g/mol, 6 Spectra/Por® membrane) against 1000 times tris buffer (10mM, 154mM ionic strength, pH = 7.4), with 3 changes of this buffer in 4h.

3.2.2. Process optimization

- ***Effect of $PBLG_{23}$-b-HYA_{10} copolymer concentration in DMSO solvent***

We investigated the effect of block copolymer concentration in DMSO in the nanoprecipitation process. Three different concentrations (0.5, 1.0 and 2.0% w/v) of block copolymer in DMSO were prepared and heated at 55°C temperature. Tris buffer was injected in block copolymer solutions at 36 mL/h (10mL syringe) by keeping the temperature at 55°C, the final concentration in block copolymer being 1mg/mL. Organic solvent (DMSO) was removed by dialysis (MWCO = 2000 g/mol, 6 Spectra/Por® membrane) against 1000 times tris buffer (10mM, 154mM ionic strength, pH = 7.4), with 3 changes of this buffer in 4h.

- ***Effect of final concentration of $PBLG_{23}$-b-HYA_{10} copolymer in nanoprecipitation***

We examined three different final concentrations (0.5, 1.0 and 2.0 mg/mL) of copolymer in the nanoprecipitation process with 1% wt of copolymer in DMSO. The block copolymer solution in DMSO was prepared and heated at 55°C. Required volumes of tris buffer were injected in the different solutions of block copolymer at 18mL/h (5ml syringe) at 55°C. Organic solvent (DMSO) was removed by dialysis (MWCO = 2000 g/mol, 6 Spectra/Por® membrane) against 1000 times tris buffer (10mM, 154mM ionic strength, pH = 7.4), with 3 changes of this buffer in 4h.

3.2.3. Effect of dilution on preformed $PBLG_{23}$-*b*-HYA_{10} vesicle

We investigated the effect of dilution on the preformed $PBLG_{23}$-*b*-HYA_{10} based vesicles. Tris buffer was injected in the DMSO solution of block copolymer (1wt %) at 36 mL/h (10 mL syringe) at 55°C. The final concentration of block copolymer was 2 mg/mL (0.2 % w/v). This concentration was slightly changed after the dialysis (1.8 mg/mL). The block copolymer dispersion was then diluted to 1.5, 1.0 and 0.5 mg/mL and analyzed by DLS.

3.2.4. Stability study

We determined the stability of polymersomes for 90 days at room temperature (RT) and at 4°C temperature. For this purpose a dispersion of polymersomes was prepared as described in paragraph 3.2.2 and divided into two batches. One batch was kept at RT with continuous slow shaking while the second batch was kept in refrigerator. Before DLS analysis, the batch from the refrigerator was vortexed for 1 min.

3.2.5. Lyophilization

Polymersomes dispersions (prepared as described in paragraph 3.2.2) were frozen with liquid nitrogen in 10 mL vials and then lyophilized (CHRIST, ALPHA 1-2 LD plus, BIOBLOCK SCIENTIFIC). After 48h, samples were removed from lyophilizer, reconstituted with 5 ml of tris buffer. Full redispersion of lyophilized vesicles was achieved only after reconstitution in tris buffer by vortex for 10min. We just used a very low power sonication bath for 30 seconds in order to accelerate the dispersion time and

eventually eliminate the few aggregates still in solution. Samples were analyzed by dynamic light scattering before and after lyophilization.

3.3. Characterization

3.3.1. Dynamic and static light scattering

Dynamic light scattering (DLS) experiments were performed using ALV Laser Goniometer, which consists of 22mW HeNe linear polarized laser with 632.8 nm wavelength and an ALV-5000/EPP Multiple Tau Digital Correlator with 125 ns initial sampling time. The samples were kept at constant temperature (25.0°C) during all the experiments. The accessible scattering angle range is from 30° up to 150°. The solutions were introduced into 10 mm diameter glass cells. The minimum sample volume required for the experiment was 1 ml. The data acquisition was done with the ALV-Correlator Control Software, and the counting time varied for each sample was 300s. Millipore water was thoroughly filtered with 0.1μm filters and directly employed for the preparation of the solutions. Dynamic light scattering measurements were evaluated by fitting of the measured normalized time autocorrelation function of the scattered light intensity. The data were fitted with the help of the constrained regularization algorithm (CONTIN), which provides the distribution of relaxation times τ, A(τ), as the inverse Laplace transform of $g_{(1)}(t)$ function

$$g_{(1)(t)} = \int_0^\infty A(\tau)\exp(-t/\tau)\, d\tau$$

Apparent diffusion coefficients D were obtained by plotting the relaxation frequency, Γ ($\Gamma = \tau^{-1}$) versus q^2, where q is the scattering vector defined as $q = (4\pi n/\lambda)\sin(\theta/2)$

$$q = \frac{4\pi n}{\lambda} \sin\left(\frac{\theta}{2}\right)$$

and λ is the wavelength of the incident laser beam (632.8 nm), θ is the scattering angle, and n is the refractive index of the medium. Single nanoparticle diffusion coefficients were determined by extrapolation to zero concentration and hydrodynamic radius (R_H) was calculated from the Stokes-Einstein relation

$$R_H = \frac{k_B T}{6\pi\eta\Gamma} q^2 = \frac{k_B T}{6\pi\eta D_{app}}$$

Where k_B is the Boltzmann constant, Γ is the relaxation frequency, T is the temperature, and η is the viscosity of the medium. The dispersity of particle sizes was then calculated by the $< \Delta\Gamma^2/\Gamma >$ in which $< \Delta\Gamma^2 >$ was determined by analysis of the first-order correlation function by cumulant analysis.

$$g_t(t)_H = \exp[-< \Gamma > t + \frac{1}{2}(\Delta\Gamma^2)t^2 - \frac{1}{6}(\Delta\Gamma^3)t^3 \pm \cdots \cdots \cdots]$$

The reduced scattering intensity was expressed in terms of Rayleigh ratios (R_θ) to derive the weight-average molecular weight (Mw) and the z-average gyration radius ($R_{G,Z}$) through the Debye equation. The ratio Kc/R_θ with $K = (4\pi^2 n_0/\lambda_0{}^4 N_A)(dn/dc)$ was determined in steps from 40° to 120° scattering angle. n_0 is the refractive index of the standard (toluene), dn/dc is the increment of the refractive index, c is the concentration, and λ_0 is the incident wavelength. Scattering intensities were calculated according to standard procedures using toluene as the standard with known absolute scattering intensity. A curvature of the angular dependence in a Zimm plot is observed in our self-assembled nanoparticles which present hydrodynamic radii larger than about 100 nm. This curvature becomes less pronounced using the Berry representation (Burchard 2005) which allows to linearize the data in some extent. The radius of gyration (R_g) and the second virial coefficient (A_2) were obtained using the equation

$$\sqrt{\frac{Kc}{R(q,c)}} = \sqrt{\frac{1}{M_W}}\left(1 + \frac{1}{6}R^2q^2\right)(1 + A_2 M_W c)$$

$(Kc/\Delta R(\theta))^{1/2}$ was plotted against $(\sin^2(\theta/2) + kC)$ (Debye equation), with k being an adjustable constant. Extrapolation of the experimental data to zero concentration and zero angle gave the M_W, R_g, and A_2.

3.3.2. Small angle neutron scattering

Small Angle Neutron Scattering (SANS) experiments were performed at the Léon Brillouin Laboratory (Orphée reactor, Saclay) on the PACE spectrometer. Two spectrometer configurations have been used in order to cover a q range from 5×10^{-3} Å^{-1} to

$0.15Å^{-1}$. The solution was introduced into 5 mm thick rectangular quartz cell. Data treatment was done with the PAsidur software (LLB). Absolute values of the scattering intensity (I(q) in cm^{-1}) were obtained from the direct determination of the number of neutrons in the incident beam and the detector cell solid angle.

3.3.3. *Freeze fracture TEM*

For freeze-fracture transmission electron microscopy (FF-TEM) experiments, a drop of the solution of $PBLG_{23}$-*b*-HYA_{10} (0.1 mg/mL) was placed between two copper planchettes of a sandwich holder and freezed by plunging into liquid propane. Sample was then fractured at -150°C and pressure of the order of 10^{-6}mBar in a BAF 300 Balzers apparatus. The fractured surfaces were replicated with platinum evaporated at a 45°angle, followed by carbon deposition normal to the fracture surface to increase mechanical strength. The copper planchettes were dissolved in chromerge® (a mixture of chromic acid, sulphuric acid and water). The detached replicas were then rinsed with water and cleaned from copolymer with DMSO, before being collected on the 200 mesh copper grid. Observations were made with a FEI Tecnai 12 Microscope working at 120keV.

3.3.4. *Atomic force microscopy*

Atomic force microscopy (AFM) was performed under air at 25°C using a Nanoscope IIIa microscope in tapping-mode. Commercially available silicon tip probes had a spring constant of 42 N m^{-1}, a resonance frequency of 285 kHz, and a typical radius of curvature in the 8-10 nm range. Both topography and phase signal images were recorded with 512 × 512 data points. All samples were prepared on mica by spin-coating at 700 rpm for 10 minutes and allowed to dry for two days at room temperature.

3.4. Results and Discussion

Solution behavior of block copolymer $PBLG_{23}$-*b*-HYA_{10} was examined by the well-known process such as direct dissolution and nanoprecipitation method. In direct dissolution at room temperature a broad relaxation time distribution was observed that could be due to the aggregation of copolymer in Tris buffer (Figure 3.2). At 40°C a sharp peak on the size distribution was observed with a polydispersity index of 0.16 obtained

from cumulant analysis. The hydrodynamic radius R_H was calculated to be 190 nm from the slope of relaxation frequency dependency to the square scattering vector.

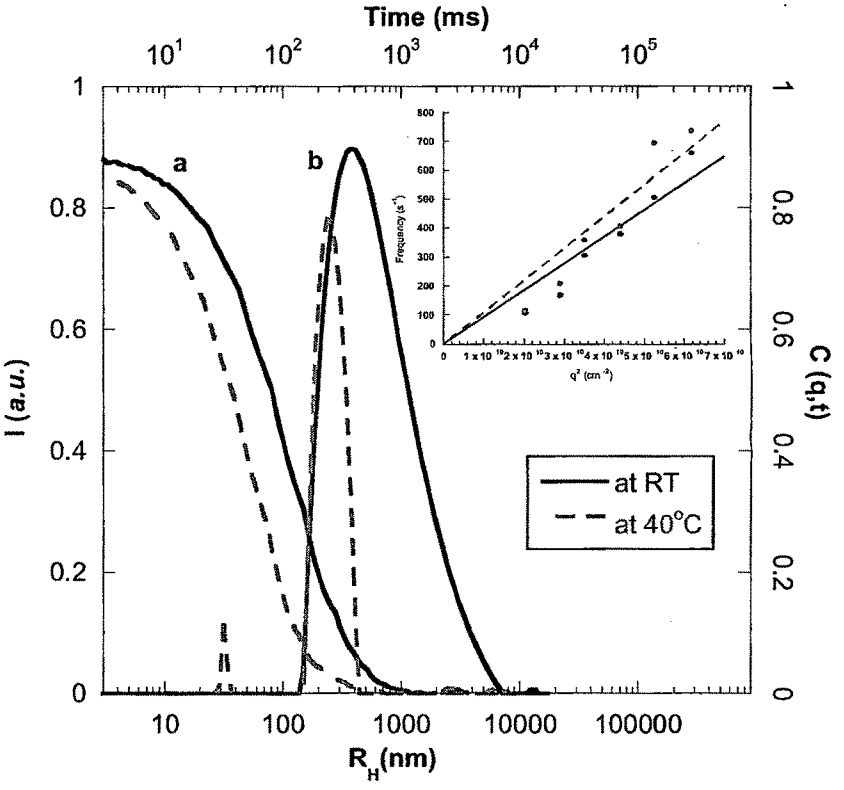

Figure 3.2 (a) DLS autocorrelation function of the $PBLG_{23}$-*b*-HYA_{10} polymersomes and (b) their time relaxation distribution at 90° scattering angle. The inset shows the relaxation frequency Γ dependency to the square scattering vector q^2. (Direct dissolution at RT and at 40°C).

In the nanoprecipitation method, tris buffer (pH = 7.4) was injected in the block copolymer solution in DMSO at 55°C. DMSO was removed by dialysis against tris buffer. DLS plot (Figure 3.3) showed one main narrow relaxation time distribution before and after dialysis. Polydispersity indexes are 0.04 and 0.08 before and after dialysis, hydrodynamic radii being 248nm and 209 nm. This decrease in size after dialysis could be due to replacement of DMSO with tris buffer (pH = 7.4).

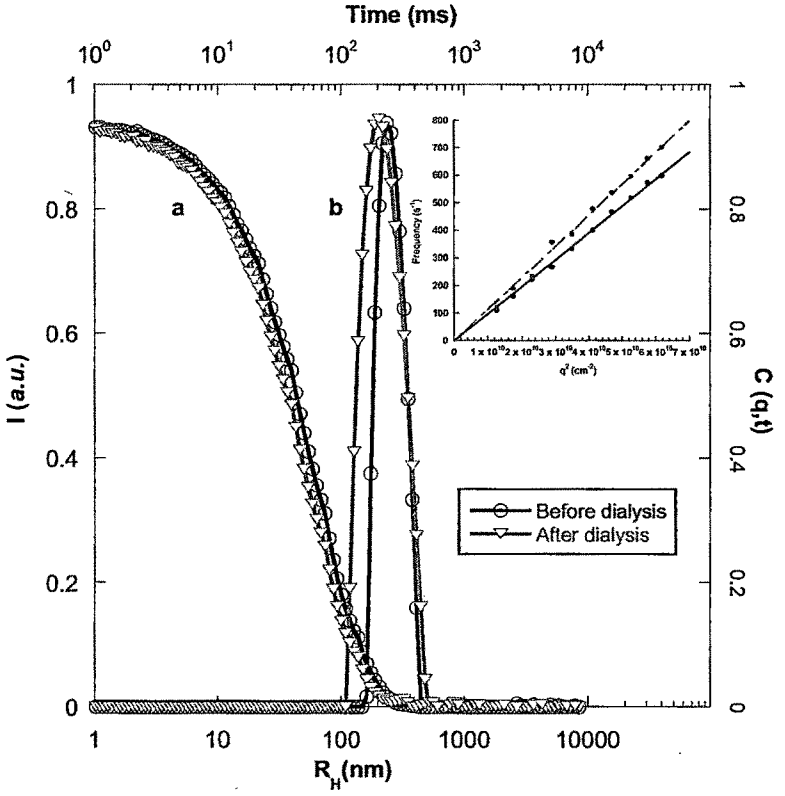

Figure 3.3 (a) DLS autocorrelation function of the PBLG$_{23}$-*b*-HYA$_{10}$ polymersomes and (b) their time relaxation distribution at 90° scattering angle. The inset shows the decay rate Γ dependency to the square scattering vector q^2. (Nanoprecipitation at 55°C).

Static light scattering measurements were also used to asses R_g/R_H. This ratio is well-known as being indicative of the morphology of the aggregates (Burchard 1983, Burchard 2005), ($R_g/R_H \sim 0.77$ for a hard sphere, $R_g/R_H = 1$ for a vesicle, $R_g/R_H = 1.7$ for a coil), provided the nanoparticles present a relatively narrow size distribution which is reasonably the case in our study. Table (3.1) represents the R_H and R_g values extracted from DLS and Berry plot analysis of SLS (Figure 3.4). Considering the light scattering results, PBLG$_{23}$-*b*-HYA$_{10}$ block copolymer would afford vesicular morphology in tris buffer ($Rg/R_H \sim 1$).

Table 3.1 Radius of Gyration (R_g), Hydrodynamic Radii (R_H), and Polydispersity Index[a]

Solvent	R_g (nm)	R_H (nm)	R_g/R_H	Expected Morphology	Dispersity Index	dn/dc
Tris Buffer	188 ±14	203	0.93	Vesicles (Polymersomes)	0.216	0.54

[a]calculated at 90° (cumulant analysis) by dynamic light scattering

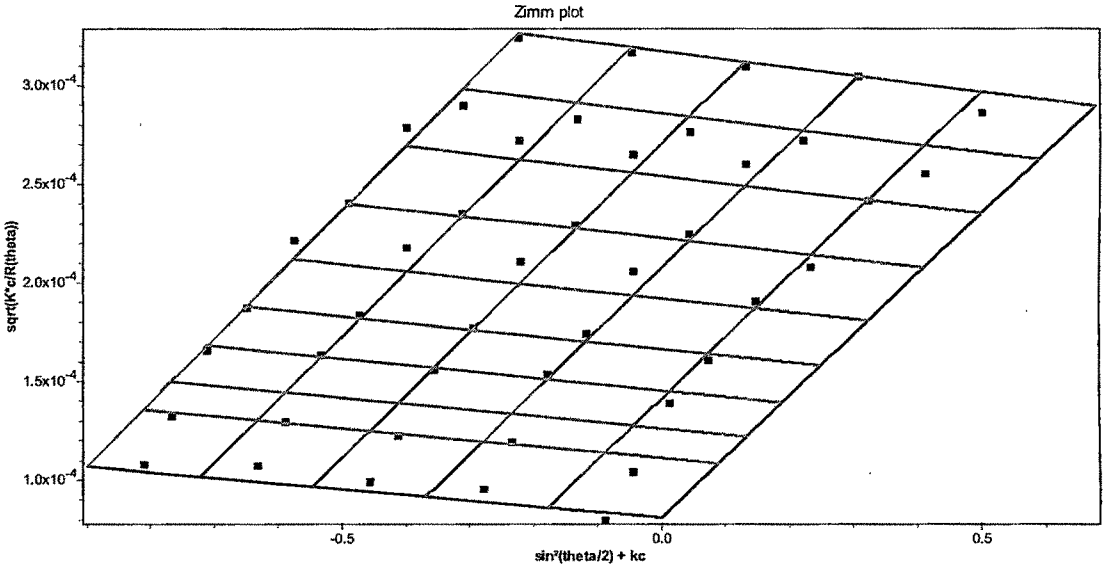

Figure 3.4 Berry plot of $PBLG_{23}$-*b*-HYA_{10} in tris buffer solvent at 25°C.

SANS experiments were also performed in order to accurately assess the vesicular morphology (Figure 3.5). The typical q^{-2} slope is together with the fitting of the scattering curve with a vesicle form factor confirming irrefutably the presence of vesicles (Cotton, 1991). In addition, from the slope of the representation $\ln(q^2I(q))$ versus q (Figure 3.5, inset) in the asymptotic Kratky-Porod approximation, we could estimate the thickness of the vesicle membrane $\delta \sim 9$nm (Chécot et al., 2005).

Assuming a bilayer structure, with PBLG blocks in α-helical conformation stacked in a strictly antiparallel orientation as in the bulk state, and HYA chains in a rod like conformation stabilizing the interface, one can calculate the expected membrane thickness using the following relation:

$$\delta = L_{PBLG} + 2Rg_{HYA}$$

We used $L_{PBLG} = 1.5 \times DP = 3.45$ nm (Calnan et al., 1991). Concerning HYA, it has been reported in literature that its persistence length in similar conditions is about 7nm. This value was derived by using both the Odijk's model from Rg vs M data and the Bohdanecky's plot from $[\eta]$ vs M data (Mendichi et al., 2003).

Considering that the characteristic length of the disaccharide repetitive unit is 1nm and that the degree of polymerisation of hyaluronan is 10, a rod conformation is assumed,

with a total length L~10nm. Therefore the radius of gyration of hyaluronan can be estimated by:

$$Rg^2=L^2/12 \qquad \text{so that} \qquad Rg\sim 2.9\text{nm}$$

Then, the total bilayer thickness is theoretically $\delta = 3.45 + (2\times 2.9) \sim 9.3$nm.

The so-calculated value is in good agreement with the experimentally determined δ value from SANS. In addition, the membrane thickness is at least two times higher than that usually obtained for liposomes, ensuring a good stability upon loading and processing. A schematic representation of the polymersome structure of $PBLG_{23}$-*b*-HYA_{10} is given on Scheme 3.1.

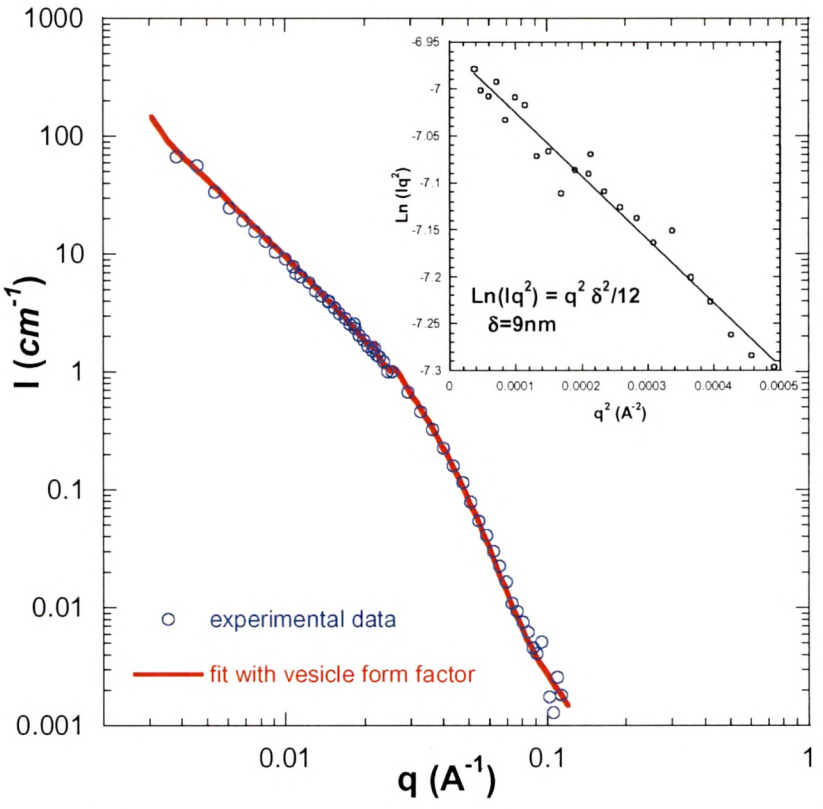

Figure 3.5 SANS of $PBLG_{23}$-*b*-HYA_{10} based polymersomes in water. Experimental data are fitted by a vesicle form factor with a radius of 220 nm, a membrane thickness (δ) of 9 nm.

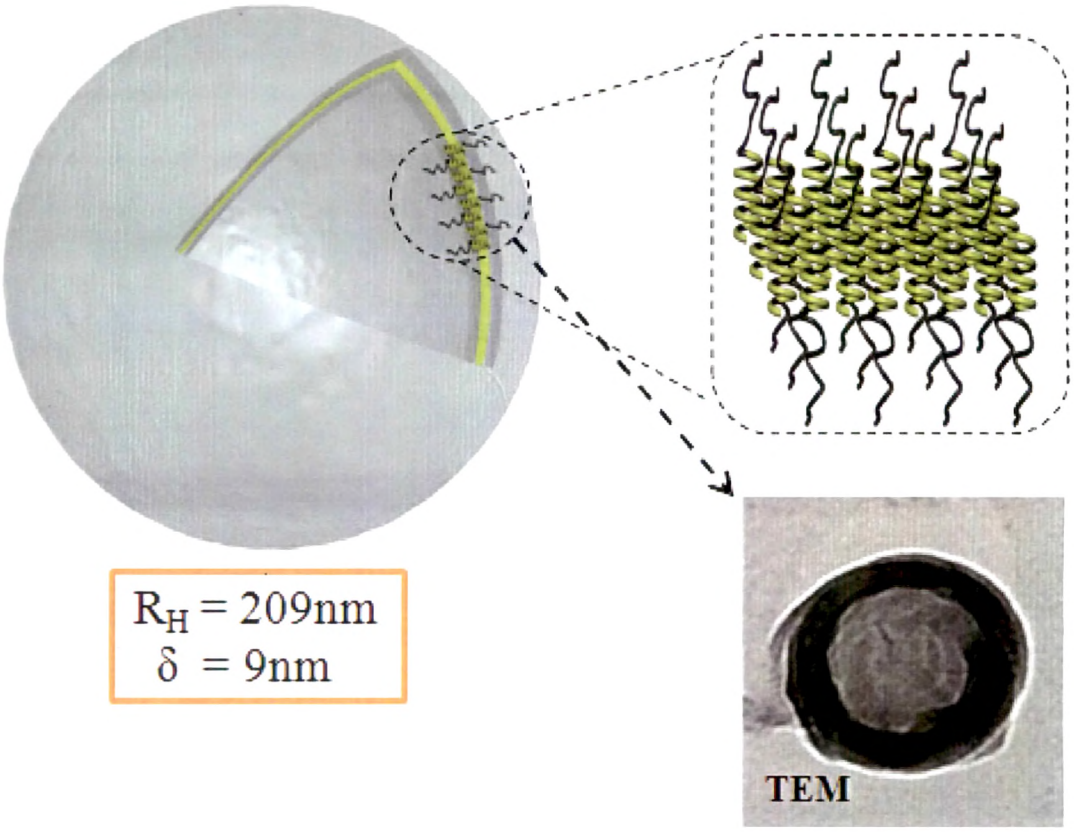

Scheme: 3.1. Schematic representation of the $PBLG_{23}$-b-HYA_{10} polymersomes, with a bilayer forming membrane with PBLG packed antiparallel

In addition, we determined some process variables such as the effect of initial copolymer concentration in DMSO, the effect of final polymer concentration in the medium and the effect of dilution on the preformed polymersomes. Different concentrations of copolymer in DMSO did not affect significantly the hydrodynamic radius in nanoprecipitation method but polydispersity increased at 2% w/v (Figure 3.6) (Table 3. 2). Polydispersity was also affected at final 0.2% w/v copolymer concentration after dialysis on fixed 1% w/v (10mg/mL) copolymer concentration in DMSO (Figure 3.7) during nanoprecipitation (Table 3.2).

Table 3.2 Effect of initial concentration of copolymer in DMSO and final concentration of copolymer in nanoprecipitation

Concentration (mg/mL) (wt %)	Hydrodynamic Radius (R_H) nm	Dispersity Index*
Effect of copolymer concentration in DMSO at 0.1 wt % of copolymer in final preparation		
5mg/mL (0.5 wt %)	156 nm	0.088
10mg/mL (1.0 wt %)	220 nm	0.098
20mg/mL (2.0 wt %)	223 nm	0.151
Effect of copolymer concentration in final preparation at 1% wt of copolymer in DMSO		
0.5mg/mL (0.05 wt %)	115 nm	0.068
1.0mg/mL (0.1 wt %)	232 nm	0.089
2.0mg/mL (0.2 wt %)	217 nm	0.159

*calculated at 90° (cumulant analysis) by dynamic light scattering

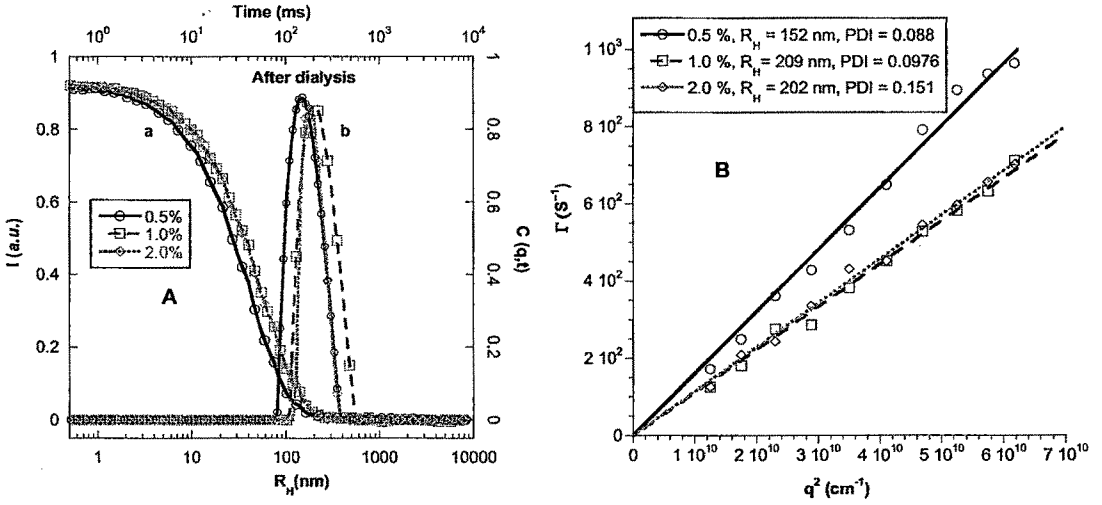

Figure 3.6 Effect of copolymer concentration in DMSO after dialysis (A) DLS autocorrelation function (a) of the $PBLG_{23}$-*b*-HYA_{10} polymersomes and (b) their time relaxation distribution at 90° scattering angle. (B) Decay rate Γ dependency to the square scattering vector q^2.

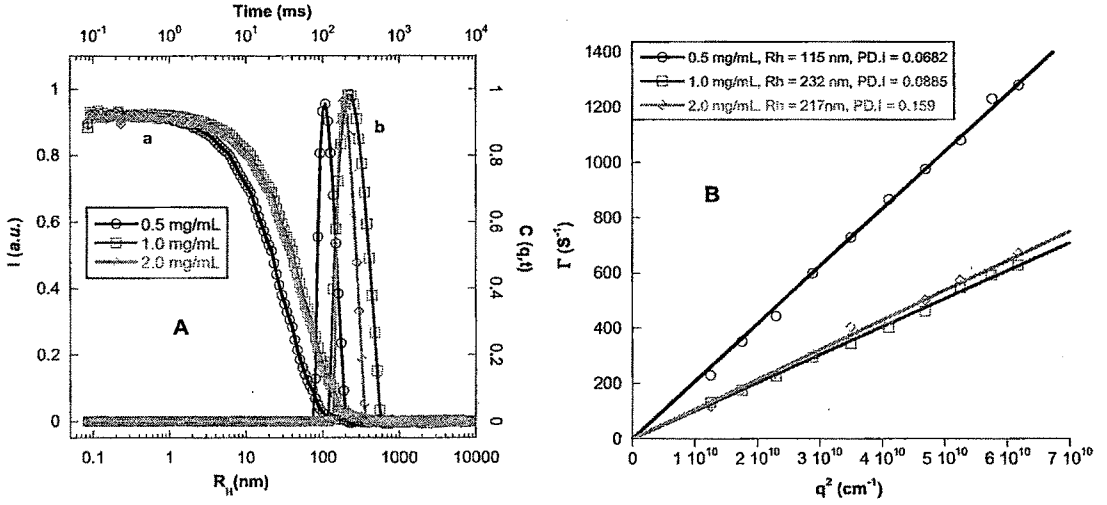

Figure 3.7 Effect of the final concentration of copolymer, after dialysis (A) DLS autocorrelation function (a) of the $PBLG_{23}$-*b*-HYA_{10} polymersomes and (b) their time relaxation distribution at 90° scattering angle. (B) Decay rate Γ dependency to the square scattering vector q^2.

Moreover, we did not see any significant changes in hydrodynamic radius of polymersomes after dilution (Figure 3.8). Once polymersomes formed, they were not affected by dilution. It is one of the ideal requirements for biological application where it will dilute more than 1000 times.

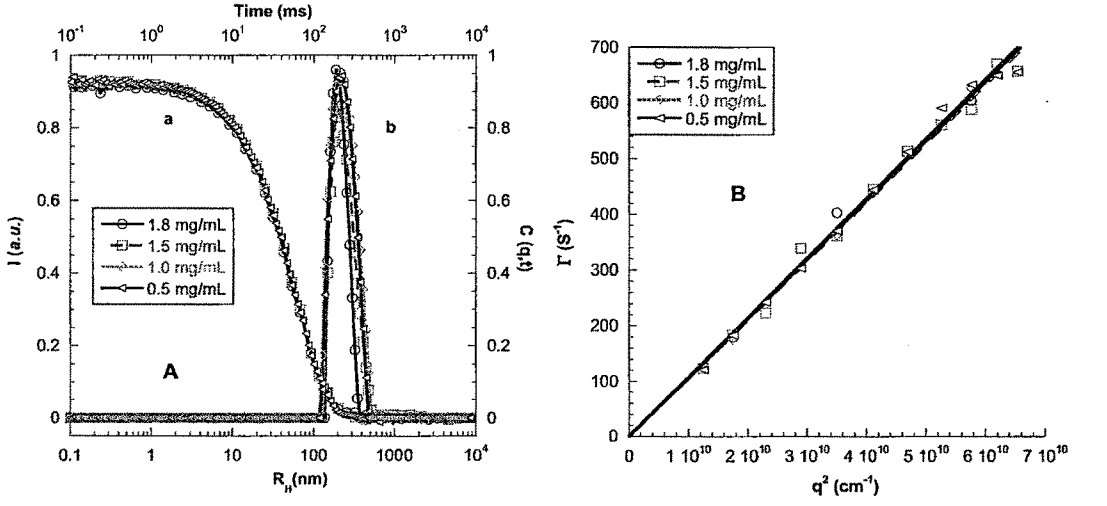

Figure 3.8 Effect of dilution on preformed polymersomes (A) DLS autocorrelation function (a) of the $PBLG_{23}$-*b*-HYA_{10} polymersomes and (b) their time relaxation distribution at 90° scattering angle. (B) Decay rate Γ dependency to the square scattering vector q^2.

In conclusion, we observed that block copolymer ($PBLG_{23}$-*b*-HYA_{10}) formed polymersomes around 200nm in hydrodynamic radius (R_H) by their intrinsic self assembly property in tris buffer (pH 7.4) through nanoprecipitation method. A radius around 120nm has been obtained after probe sonication (130 watt, 20 kHz, Vibra Cell, 75186, 60% amplitude, pulse program: 2 second on/1 second off for 2-3 minutes. Furthermore, polymersomes stability was examined at different pHs for their particle size and surface charge potential (Figure 3.9). Particle sizes were not affected from pH 9 to pH 3 but below pH 3 particle sizes increased due to their aggregation. The zeta potential did not vary from pH 9 to pH 4 but below pH 4, the zeta potential started to increase and almost neutral surface charge was obtained at pH 2.0. This is in good agreement with the known pka value for hyaluronan (pKa =3) (Liao et al., 2005).

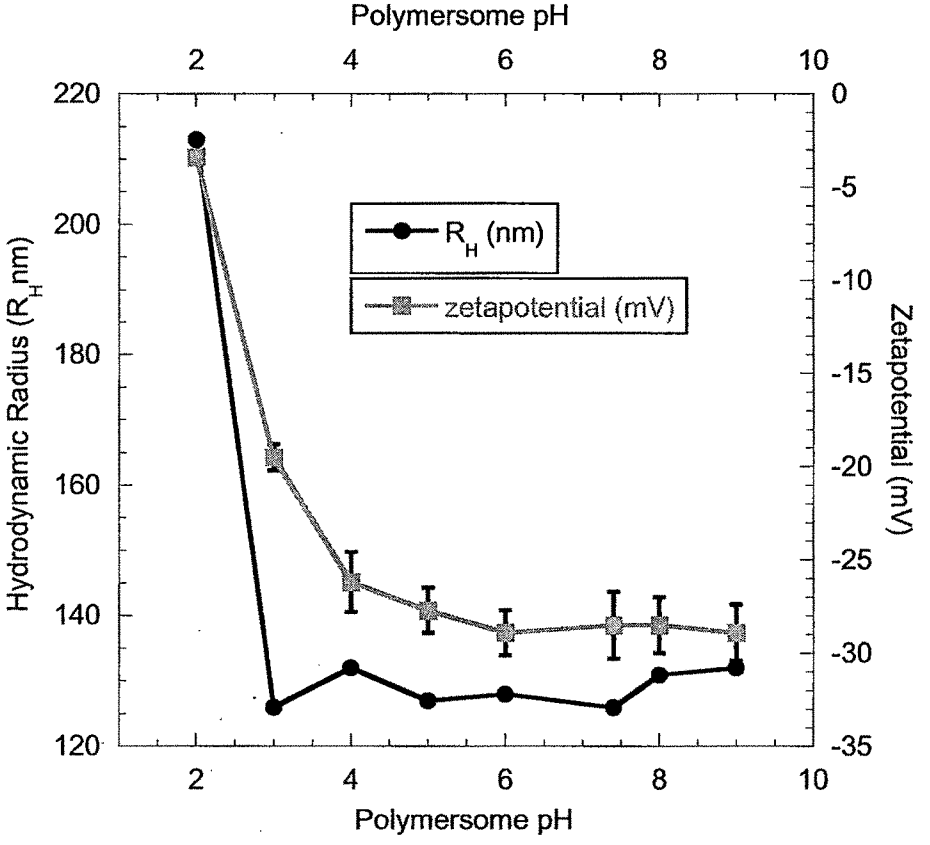

Figure 3.9 Effect of pH on the surface potential and hydrodynamic radius of polymersomes obtained by sonication.

Together with light and small angle neutrons scattering techniques (DLS, SLS and SANS), transmission electron (TEM) and atomic force microscopy (AFM) imaging were also used to attest the obtained vesicular morphology. Figure 3.10 reveals typical morphology of polymersomes by TEM and FF-TEM. Whole images show typical images of polymersomes. The characteristic sizes are in rather good agreement with the hydrodynamic sizes obtained by DLS measurements. Figure 3.11 represent the AFM image of polymersomes prepared by nanoprecipitation and one can clearly see the soft hydrophilic hyaluronan shell, spreading around the polymersomes and strongly adsorbing onto the hydrophilic mica surface.

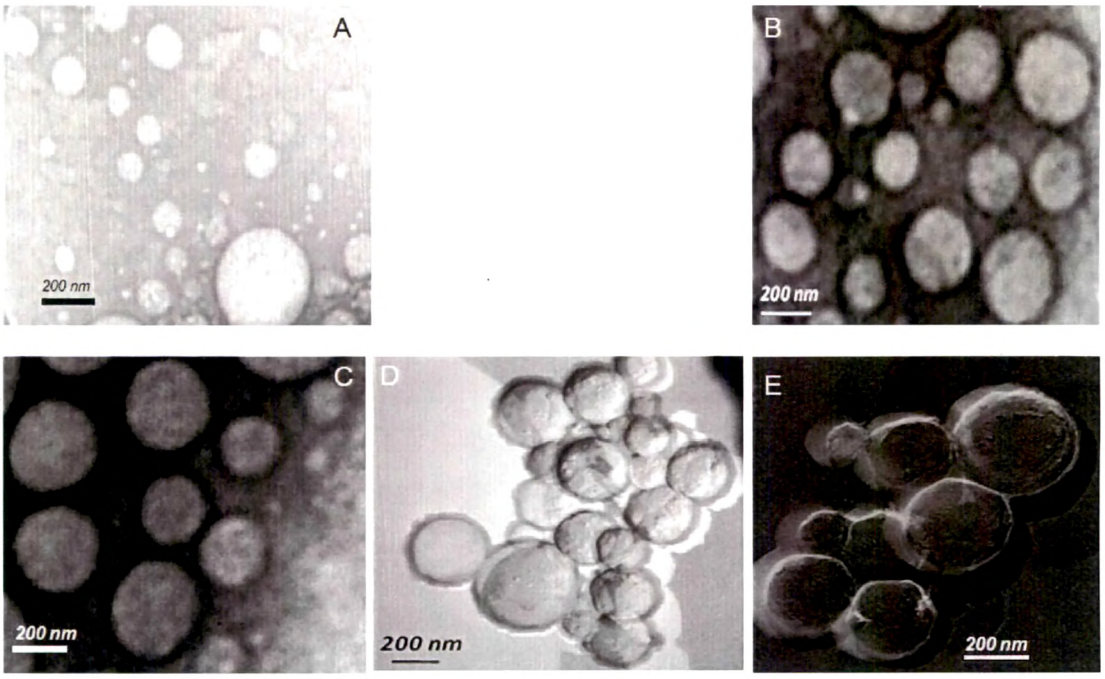

Figure 3.10 TEM and FF-TEM images of $PBLG_{23}$-*b*-HYA_{10}. (A) TEM images of the samples prepared by direct dissolution at 40^0C and (B, C) TEM images (D, E) FF-TEM images of samples prepared by nanoprecipitation at 55^0C.

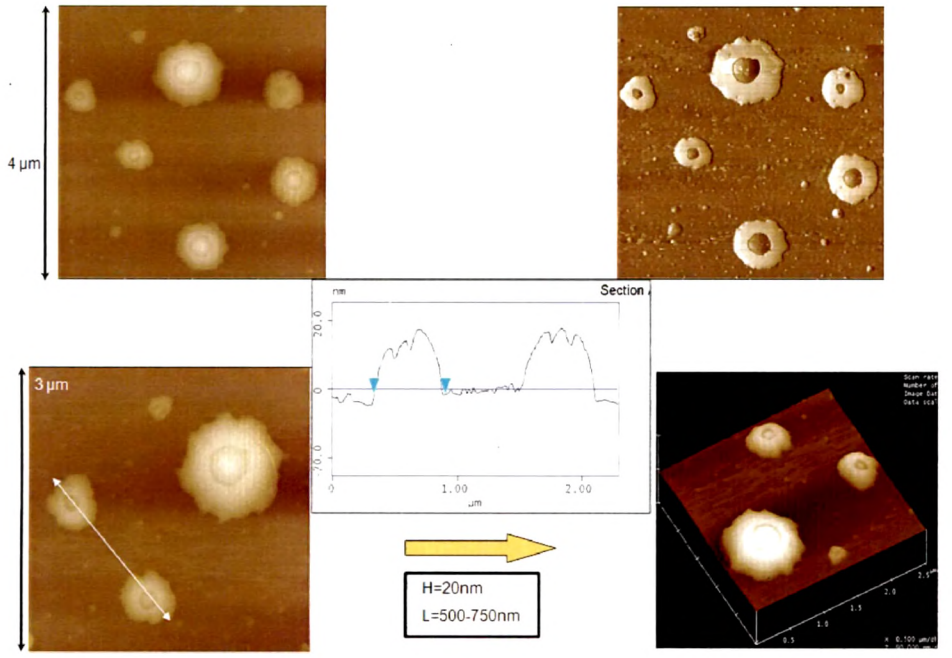

Figure 3.11 AFM imaging of $PBLG_{23}$-*b*-HYA_{10} in tris buffer.

Attractive properties of block copolymer over the lipids make polymersomes more stable than liposomes. As we have already discussed above the polymersomes were not affected by the dilution which is a crucial point when they will used for pharmaceutical applications. Figure 3.12 demonstrated the stability of polymersome for 90 days at RT and at 4°C. Polymersomes may form loose aggregates which can easily be broken by vortexing. This slight aggregation could be due to the polyelectrolyte character of hyaluronan.

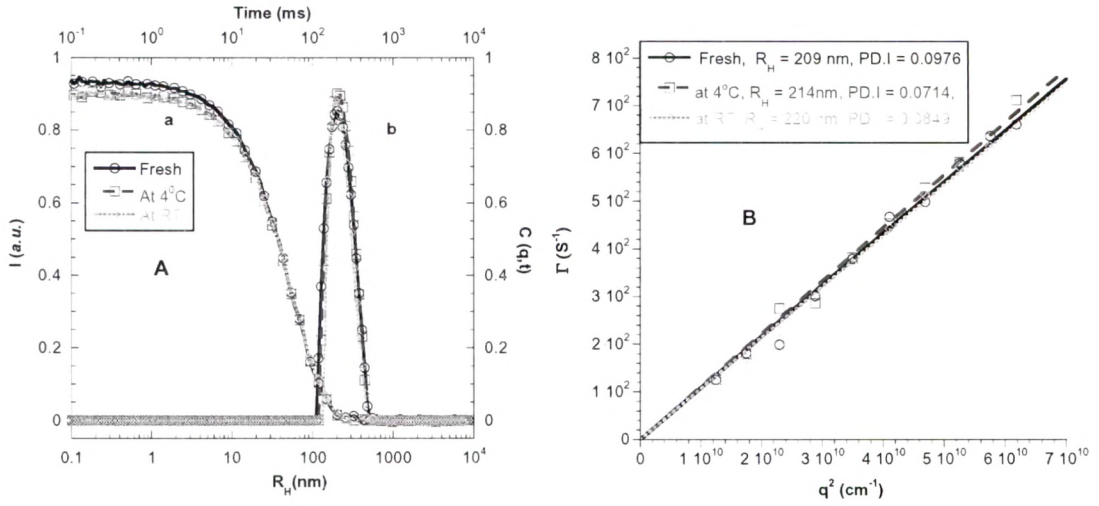

Figure 3.12 Stability of polymersomes after 90 days (A) DLS autocorrelation function (a) of the $PBLG_{23}$-b-HYA_{10} polymersomes and (b) their time relaxation distribution at 90° scattering angle. (B) Decay rate Γ dependency to the square scattering vector q^2.

In liposomes, the composition of the lipid bilayer and the aqueous phase, the amount of the external water, the bilayer–drug interaction and storage conditions are the main factors influencing liposomes stability (Sarbolouki and Toliat, 1998; Brandl, 2001). Therefore, lyophilization is widely used to enhance the stability of proteins, peptides, and liposomal/nanoparticles dispersions (Wang 2000; Glavas-Dodov et al., 2005; Pozo-Rodríguez et al., 2009). Therefore, we have investigated the lyophilization effect on polymersomes. Figure 3.13 shows some images before and after the reconstitution of freeze dried polymersomes in tris buffer (pH 7.4).

Figure 3.13 Images of polymersomes before and after lyophilization.

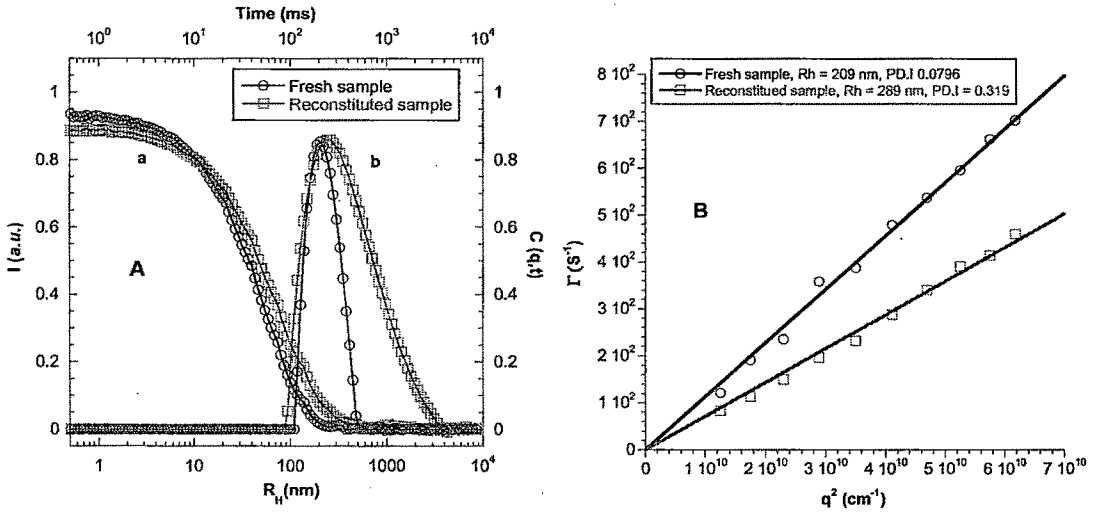

Figure 3.14 Lyophilization effect (A) DLS autocorrelation function (a) of the $PBLG_{23}$-*b*-HYA_{10} polymersomes and (b) their time relaxation distribution at 90° scattering angle. (B) Decay rate Γ dependency to the square scattering vector q^2.

Figure 3.14 shows that polymersomes were easily reconstituted from the freeze dried powder with tris buffer trough vortexing for few minutes (10 min). A slight increase in R_H and in dispersity is observed. Interestingly this increase is far below what is observed for reconstituted liposomes after lyophilisation where sizes may increase more than 10 times (Peer et al., 2003). The ease to lyophilize and redisperse polymersomes may be linked to the cryoprotective capacity of hyaluronan as for most of the sugars and polysaccharides (Wang, 2000; Peer et al., 2003). In our formulation, we have 40 wt% fraction of hyaluronan, therefore any additional cryoprotectant is not required. It is an additional favorable feature of $PBLG_{23}$-*b*-HYA_{10} polymersomes for enhancement of long term stability of proteins and drugs.

3.5. Conclusion

$PBLG_{23}$-*b*-HYA_{10} nanoparticles were prepared by direct dissolution and nanoprecipitation method. All the results obtained by the mean of different techniques (DLS, SLS, SANS AFM, TEM) evidenced vesicular morphologies. Well-defined polymersomes were obtained by the nanoprecipitation method which requires a low initial concentration of copolymer in DMSO and a low final concentration of copolymer in tris buffer. They are stable in a large pH range (3 to 9) and upon dilution. Moreover

they present a good stability over time at room temperature or at 4°C (Refrigerator storage). Due to the presence of hyaluronan chains (40 wt%), polymersomes were easily redispersed after lyophilization without affecting their sizes. This chapter has revealed that well-defined and stable polymersomes could be obtained in aqueous media under optimized conditions and also well-controlled lyophilization conditions could be suitable to use polymersomes as drug carriers in anticancer therapy.

References

- Ahmed F, Discher DE. Self-porating polymersomes of PEG-PLA and PEG-PCL: Hydrolysis-triggered controlled release vesicles. Journal of Controlled Release 2004;96(1),37-53.
- Ahmed F, Pakunlu RI, Srinivas G, Brannan A, Bates FS, Klein ML, 140. Minko T, Discher DE. Shrinkage of a Rapidly Growing Tumor by Drug-loaded Polymersomes: pH-triggered release through copolymer degradation. Mol Pharma 2006;3(3):340–50.
- Brandl M. Liposomes as drug carriers: A technological approach. Biotechnology Annual Review 2001;7,59-85.
- Burchard W. In Polysaccharides: Structural Diversity and Functional Versatility, 2nd edition; Dimitriu, S., Ed.; Marcel Dekker: New York, 2005; pp 189-236.
- Burchard W. Static and dynamic light scattering from branched polymers and biopolymers. AdV Polym Sci 1983;48,1–124.
- Burke S, Shen H, Eisenberg A. Polymer crystallization in complex conditions. Towards more realistic modelling of industrial processes. Macromolecular Symposia 2001;175,225-38.
- Calnan BJ, Tidor B, Biancalana S, Hudson D, Frankel AD. Arginine-mediated RNA recognition: The arginine fork. Science 1991;252 (5010), 1167-71.
- Chécot F, Brulet A, Oberdisse J, Gnanou Y, Mondain Monval O, 63. Lecommandoux S. Structure of polypeptide-based diblock copolymers in solution: stimuli-responsive vesicles and micelles. Langmuir 2005;21(10):4308–15.

- Chécot F, Lecommandoux S, Gnanou Y, Klok H-A. Water soluble 61. stimuli-responsive vesicles from peptide-based diblock copolymers. Angew Chem Int. Ed 2002;114(8):1395–9.
- Choucair A, Eisenberg A. Control of amphiphilic block copolymer morphologies using solution conditions. European Physical Journal E 2003;10(1),37-44.
- Cornelissen JJLM, Fischer M, Sommerdijk NAJM, Nolte RJM. Helical superstructures from charged poly(styrene)- poly(isocyanodipeptide) block copolymers. Science 1998;280(5368),1427-30.
- Cotton JP. in *Neutron, X-Ray and Light Scattering*, Eds: P.Lindner, T. Zemb, Elsevier Science Publishers B.V., North-Holland, 1991, p.19.
- del Pozo-Rodríguez A, Solinís MA, Gascón AR, Pedraz JL. Short- and long-term stability study of lyophilized solid lipid nanoparticles for gene therapy. European Journal of Pharmaceutics and Biopharmaceutics 2009;71(2),181-89.
- Dimova R, Seifert U, Pouligny B, Förster S, Döbereiner H-G. Hyperviscous diblock copolymer vesicles. European Physical Journal E 2002;(3),241-50.
- Ding J, Liu G. Polyisoprene-block-poly(2-cinnamoylethyl methacrylate) vesicles and their aggregates. Macromolecules 1997;30(3),655-57.
- Discher BM, Hammer DA, Bates FS, Discher DE. Polymer vesicles in various media. Current Opinion in Colloid and Interface Science 2000;5(1-2),125-31.
- Discher BM, Won Y-Y, Ege DS, Lee JC-M, Bates FS, Discher DE, Hammer DA. Polymersomes: Tough vesicles made from diblock copolymers. Science 1999;284(5417),1143-46.
- Discher DE, Eisenberg A. Polymer vesicles. Science 2002;297(5583),967-73.
- Glavas-Dodov M, Fredro-Kumbaradzi E, Goracinova K, Simonoska M, Calis S, Trajkovic-Jolevska S, Hincal AA. The effects of lyophilization on the stability of liposomes containing 5-FU. International Journal of Pharmaceutics 2005;291(1-2),79-86.

- Holder SJ, Hiorns RC, Sommerdijk NAJM, Williams SJ, Jones RG, Nolte RJM. The first example of a poly(ethylene oxide)-poly(methylphenylsilane) amphiphilic block copolymer: Vesicle formation in water. Chemical Communications 1998;(14),1445-46.
- Kim Y, Tewari M, Pajerowski JD, Cai S, Sen S, Williams J, Sirsi S, Lutz G, Discher DE. Polymersome delivery of siRNA and antisense oligonucleotides. J Control Release 2009 Mar 4;134(2):132-40.
- Kukula H, Schlaad H, Antonietti M, Forster S. The formation of polymer vesicles or "peptosomes" by polybutadiene-block-poly(L-glutamate)s in dilute aqueous solution. J Am Chem Soc 2002;124(8):1658–63.
- Lee James C-M, Bermudez H, Discher BM, Sheehan MA, Won Y-Y, Bates FS, Discher DE. Preparation, stability, and in vitro performance of vesicles made with diblock copolymers. Biotechnology and Bioengineering 2001;73(2),135-45.
- Levine DH, Ghoroghchian PP, Freudenberg J, Zhang G, Therien MJ, Greene MI, Hammer DA, Murali R. Polymersomes: a new multi-functional tool for cancer diagnosis and therapy. Methods 2008;46(1):25-32.
- Li Z-C, Jin W, Li F-M. Vesicles prepared from amphiphilic copolymers. Reactive and Functional Polymers 1999;42(1),21-30.
- Liao YH, Jones SA, Forbes B, Martin GP, Brown MB. Hyaluronan: pharmaceutical characterization and drug delivery. Drug Deliv 2005;12(6):327-42.
- Mendichi R, Soltés L, Giacometti SA. Evaluation of radius of gyration and intrinsic viscosity molar mass dependence and stiffness of hyaluronan. Biomacromolecules 2003;4(6),1805-10.
- Nardin C, Hirt T, Leukel J, Meier W. Polymerized ABA triblock copolymer vesicles. Langmuir 2000;16(3),1035-41.
- Nardin C, Hirt T, Leukel J, Meier W. Polymerized ABA triblock copolymer vesicles. Langmuir 2000;16 (3),1035-41.

- Nardin C, Widmer J, Winterhalter M, Meier W. Amphiphilic block copolymer nanocontainers as bioreactors. European Physical Journal E 2001; 4(4),403-410.
- Peer D, Florentin A, Margalit R. Hyaluronan is a key component in cryoprotection and formulation of targeted unilamellar liposomes. Biochimica et Biophysica Acta - Biomembranes 2003;1612(1),76-82.
- Photos PJ, Bacakova L, Discher B, Bates FS, Discher DE. Polymer vesicles in vivo: Correlations with PEG molecular weight. Journal of Controlled Release 2003;90(3),323-34.
- Sarbolouki MN, Toliat T. Storage stability of stabilized MLV and REV liposomes containing sodium methotrexate (aqueous and lyophilized). PDA Journal of Pharmaceutical Science and Technology 1998;52(1),23-27.
- Schillén K, Yekta A, Ni S, Farinha JPS, Winnik MA. Characterization of polyisoprene-b-poly(methyl methacrylate) diblock copolymer micelles in acetonitrile. Journal of Physical Chemistry B 1999;103(43),9090-03.
- Schulén K, Bryskhe K, Mel'Nikova YS. Vesicles formed from a poly(ethylene oxide)-poly(propylene oxide)-poly(ethylene oxide) triblock copolymer in dilute aqueous solution. Macromolecules 1999;32(20),6885-88.
- Shen H, Eisenberg A. Block length dependence of morphological phase diagrams of the ternary system of PS-b-PAA/dioxane/H2O. Macromolecules 2000;33(7),2561-72.
- Upadhyay K, Agrawal H, Upadhyay C, Schatz C, Le Meins J, Misra A, Lecommandoux S. Role of block copolymer nanoconstructs in cancer therapy. Crit Rev Ther Drug Carrier Syst 2009;26(2):157-205.
- Wang W. Lyophilization and development of solid protein pharmaceuticals. International Journal of Pharmaceutics 2000;203(1-2),1-60.
- Yu G-E, Eisenberg A. Multiple morphologies formed from an amphiphilic ABC triblock copolymer in solution. Macromolecules 1998;31(16),5546-49.

- Yu K, Eisenberg A. Bilayer morphologies of self-assembled crew-cut aggregates of amphiphilic PS-b-PEO diblock copolymers in solution. Macromolecules 1998;31(11),3509-18.
- Yu K, Eisenberg A. Multiple morphologies in aqueous solutions of aggregates of polystyrene-block-poly(ethylene oxide) diblock copolymers. Macromolecules 1996;29 (19), 6359-61.
- Yu Y, Zhang L, Eisenberg A. Morphogenic effect of solvent on crew-cut aggregates of apmphiphilic diblock copolymers. Macromolecules 1998;31(4),1144-54.
- Zhang L, Eisenberg A. Multiple morphologies and characteristics of 'crew-cut' micelle-like aggregates of polystyrene-b-poly(acrylic acid) diblock copolymers in aqueous solutions. Journal of the American Chemical Society 1996;118(13),3168-81.
- Zhang L, Eisenberg A. Multiple morphologies of 'crew-cut' aggregates of polystyrene-b-poly(acrylic acid) block copolymers. Science 1995;268(5218),1728-45.